HAL
open science

Wetting of Ga Droplets in SiO 2 /Si Cavities: Application to Self-Assisted GaAs Nanowire Growth

Louis Bailly-Salins, Marco Vettori, Thomas Dursap, Philippe Regreny, Gilles Patriarche, Michel Gendry, José Penuelas, Alexandre Danescu

To cite this version:

Louis Bailly-Salins, Marco Vettori, Thomas Dursap, Philippe Regreny, Gilles Patriarche, et al.. Wetting of Ga Droplets in SiO 2 /Si Cavities: Application to Self-Assisted GaAs Nanowire Growth. Crystal Growth & Design, 2022, 22 (10), pp.6070-6078. 10.1021/acs.cgd.2c00685 . hal-04106867

HAL Id: hal-04106867

https://hal.science/hal-04106867v1

Submitted on 26 May 2023

HAL is a multi-disciplinary open access archive for the deposit and dissemination of scientific research documents, whether they are published or not. The documents may come from teaching and research institutions in France or abroad, or from public or private research centers.

L'archive ouverte pluridisciplinaire **HAL**, est destinée au dépôt et à la diffusion de documents scientifiques de niveau recherche, publiés ou non, émanant des établissements d'enseignement et de recherche français ou étrangers, des laboratoires publics ou privés.

Distributed under a Creative Commons Attribution 4.0 International License

CRYSTAL GROWTH & DESIGN

pubs.acs.org/crystal Article

Wetting of Ga Droplets in SiO_2/Si Cavities: Application to Self-Assisted GaAs Nanowire Growth

Louis Bailly-Salins, Marco Vettori, Thomas Dursap, Philippe Regreny, Gilles Patriarche, Michel Gendry, José Penuelas, and Alexandre Danescu*

Cite This: https://doi.org/10.1021/acs.cgd.2c00685 Read Online

ACCESS | Metrics & More | Article Recommendations

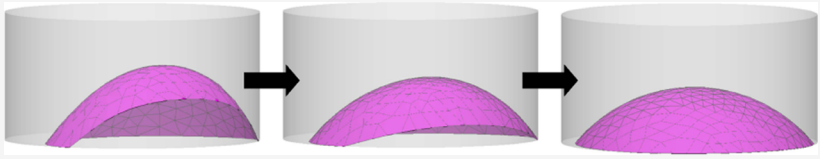

ABSTRACT: In this paper, we compute and compare the surface energy of various Ga liquid droplets wetting a cylindrical cavity in various configurations. While for some of these configurations, the surface energy can be computed explicitly; for others, numerical computation is needed. Motivated by the results obtained for the cylindrical cavities, we explore the case of the more realistic situation, conical cavities. Our results provide a relation between the geometry of the conical cavity and the equilibrium wetting angles of the droplet on the bottom and on the sidewall of the cavity, which insures the dewetting of the lateral surface. This is an important result toward the control of the verticality during nanowire growth by the vapor−liquid−solid method.

Downloaded via Alexandre Danescu on September 21, 2022 at 18:35:33 (UTC).
See https://pubs.acs.org/sharingguidelines for options on how to legitimately share published articles.

1. INTRODUCTION

Nanowires (NWs) are promising building blocks for many functional devices thanks to their exceptional properties.[1] The most popular NW growth method is based on the vapor−liquid−solid (VLS) mechanism.[2] The VLS mechanism consists of the formation of a solid phase due to the saturation of liquid droplets, which are exposed to a vapor phase. The droplets are usually randomly deposited on a solid surface resulting in a random organization of the NWs.[3] However, in order to benefit from collective effects, like in photonic crystals,[4] it is necessary to fabricate periodic arrays of NWs. Moreover, achieving patterned growth of NWs is a good way to optimize their size distribution and their physical properties.[5] As a consequence, a key issue for many applications is to fabricate organized patterns of particle catalyst nanoparticles on the surface that will act as nucleation seeds for the VLS NW growth. Although the fabrication of such periodic arrays of metallic nanoparticles has been investigated for years,[6−8] it is still a challenge to achieve low cost and large area patterns. These patterns are usually fabricated by lithography techniques, which allow one to obtain periodic arrays of holes on a surface. Then, under appropriate experimental conditions the liquid droplets can be deposited in the holes and be exposed to the vapor phase. However, experimental results reported in the literature highlight the complexity of the NW nucleation when the liquid droplet is confined in patterned holes.[8] In particular, one can assume that the shape of the liquid droplet, its surface energy,[9] and the wetting on the hole surfaces have a strong impact of the first steps of the crystal nucleation. Although recent experimental advances in characterization methods, such as in situ transmission electron microscopy(TEM), allow one to provide a better picture of the VLS mechanism,[10,11] a clear description of the mechanism of NW nucleation in a cavity is still missing. Moreover, only few studies reported theoretical explanation of the wetting of liquid in holes with geometry corresponding to those of the patterned substrates. In this article, we studied the wetting of a liquid droplet in cylindrical and conical cavities. Various wetting configurations as well as hole geometries were considered and their corresponding surface energy was calculated in order to give a clear picture of the phenomena involved during the first steps of the VLS growth on patterned substrates. Applied to the particular case of a Ga droplet in a SiO_2/Si conical cavity, the results obtained are in excellent agreement with our experiments[12] and pave the way to a better control of the NW verticality on patterned substrates.[13]

2. SURFACE ENERGY AND DROPLET CONFIGURATIONS

The presence of the droplet in the cylindrical cavity replaces some of solid/vapor interfaces by solid/liquid interfaces and creates a new liquid/vapor interface. Thus, it seems natural to associate to a given morphology of the droplet the

Received: June 20, 2022
Revised: September 7, 2022

 © XXXX American Chemical Society

corresponding variation of the surface energy, further denoted as ΔW, and defined as the surface energy of the system in the presence of the droplet minus the reference surface energy of the cavity without the droplet. This gives

$$\Delta W = A_{VL}\gamma_{VL} + A_{LS}(\gamma_{LS} - \gamma_{SV}) \tag{1}$$

where A_{LV} and A_{LS} are the areas of the vapor/liquid and liquid/solid interfaces, respectively, and γ_{VL}, γ_{LS}, and γ_{SV} are the surface energies of the vapor/liquid, the liquid/solid, and the solid/vapor interfaces, respectively. In 1, the first term accounts for the newly created vapor/liquid interface and the second term accounts for the area of the liquid/solid interface that replaces various solid/vapor (bottom and/or wall) interfaces.

For generality, we shall consider here the generic situation in which the wetting angles of the droplet on the bottom (θ_b) and the walls (θ_w) of the cavity, respectively, are different. This is for instance the case when one discusses liquid droplets in cavities formed in a thin SiO_2 layer on crystalline Si. Using the Young's relation for each of the solid/vapor interface, we can rewrite 1 as

$$\Delta W = \gamma_{VL}(A_{VL} - A_{LS}^{(b)} \cos\theta_b - A_{LS}^{(w)} \cos\theta_w) \tag{2}$$

where $A_{LS}^{(b)}$ denotes the area of the liquid/solid interface located at the bottom of the cavity and $A_{LS}^{(w)}$ is the area of the liquid/solid interface between the droplet and the wall. For later references, $A_{LS} = A_{LS}^{(b)} + A_{LS}^{(w)}$ denotes the total area of the solid/drop interface. Notice that our definition in 2 is independent of the droplet morphology and satisfies $\Delta W = 0$ when the droplet is absent.

Depending on the position of the droplet in the cavity, using notations in ref 8, we define several different configurations (Figure 1 illustrates these in the case of the cylindrical cavity):

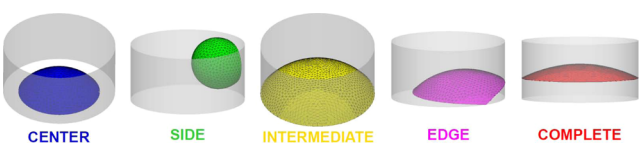

Figure 1. Liquid/vapor interface for morphologically different configurations of a droplet in a cylindrical cavity. From left to right: CENTER, SIDE, INTERMEDIATE, EDGE, and COMPLETE. The color code adopted here will be conserved for all subsequent graphics.

- In a CENTER configuration, the droplet wets only the bottom of the cavity at wetting angle θ_b.
- In a SIDE configuration, the droplet wets only the wall of the cavity at wetting angle θ_w.
- In an INTERMEDIATE configuration, all of the bottom of the cavity is wet but not the wall, so that the droplet is pinned at the line between the bottom and the wall. In this situation (see Gibbs[14]), the droplet has a volume-dependent contact angle θ_i such that

$$\min\left(\theta_b, \theta_w - \frac{\pi}{2}\right) \le \theta_i \le \max\left(\theta_b, \theta_w - \frac{\pi}{2}\right)$$

- In an EDGE configuration, the droplet wets partially both the bottom and the wall of the cavity.
- In a COMPLETE configuration, all of the bottom of the cavity is wet and the triple line lies strictly above the cavity basis.

Obviously, the INTERMEDIATE configuration exists only if $\max(\theta_b, \theta_w - \pi/2) > \min(\theta_b, \theta_w - \pi/2)$ and can be seen as a transition between the CENTER and COMPLETE configurations. In particular, if $\theta_b = \theta_w$, the INTERMEDIATE configuration exists for an angle interval of $\pi/2$. Clearly, all configurations defined above exist only for (relative) volumes in specific intervals described below.

3. DROPLET IN A CYLINDRICAL CAVITY

Given the surface tensions or equivalent, the contact angles θ_b and θ_w, by using elementary geometry, one can compute explicitly ΔW for the three of the above configurations: CENTER, INTERMEDIATE, and COMPLETE. Indeed, for the CENTER and INTERMEDIATE configurations, the droplet shape of minimum surface energy is that of a spherical cap, while for the COMPLETE configuration a spherical cap placed on a cylinder. Thus, its area is known, so is its surface energy.

We shall discuss first the case $\theta_b < \pi/2$ and $\theta_w > \pi/2$ (which is that of a cylindrical cavity in an SiO_2 layer on a Si substrate). In this case, we have:

- The CENTER configuration: this is a spherical cap and exists only if the volume of droplet V is such that $0 < V < V(R, \theta_b)$ where the function

$$V(r, \theta) = \frac{\pi r^3(1 - \cos\theta)^2(2 + \cos\theta)}{3 \sin^3\theta}$$

gives the volume of a spherical cap with basis radius r and wetting angle θ. In this configuration, we have

$$\begin{aligned}\frac{\Delta W}{\gamma_{VL}} &= A_{VL} - \cos\theta_b A_{LS} \\ &= A_{VL}\left(1 - \cos\theta_b \frac{1 + \cos\theta_b}{2}\right) \\ &= 2\left(\frac{3V}{2 + \cos\theta_b}\right)^{2/3}\left(\frac{\pi}{1 - \cos\theta_b}\right)^{1/3} (2 - \cos\theta_b - \cos^2\theta_b) \\ &= V^{2/3}[36\pi(2 + \cos\theta_b) \sin^4(\theta_b/2)]^{1/3}\end{aligned} \tag{3}$$

We notice that $\lim_{V\to 0} \Delta W = 0$ as expected.

- The INTERMEDIATE configuration: $\theta_m = \min(\theta_b, \theta_w - \pi/2)$, $\theta_M = \max(\theta_b, \theta_w - \pi/2)$, $V_m = V(R, \theta_m)$ and $V_M = V(R, \theta_M)$. This configuration is also a spherical cap and exists only if the volume of the droplet lies in interval $[V_m, V_M]$. In this case, we have

$$\frac{\Delta W}{\gamma_{VL}} = 2\left(\frac{3V}{2 + \cos\theta}\right)^{2/3}\left(\frac{\pi}{1 - \cos\theta}\right)^{1/3} - \pi R^2 \cos\theta_b \tag{4}$$

where θ is the unique positive solution in the interval $[\theta_m, \theta_M]$ of the equation $V(R, \theta) = V$.

- The COMPLETE configuration is a spherical cap on a cylinder and exists if the droplet volume lies in the interval $[V_M, V_M + \pi h R^2]$. In this case

$$\frac{\Delta W}{\gamma_{VL}} = 2\left(\frac{3V}{2 + \cos\theta_M}\right)^{2/3}\left(\frac{\pi}{1 - \cos\theta_M}\right)^{1/3} - \pi R^2 \cos\theta_b - 2\pi R h \cos\theta_w \tag{5}$$

https://doi.org/10.1021/acs.cgd.2c00685
Cryst. Growth Des. XXXX, XXX, XXX−XXX

A straightforward computation shows that ΔW defined in 3−5 is a continuous function. Let the aspect ratio of the cylindrical cavity be defined as R/h. Figure 2 shows the

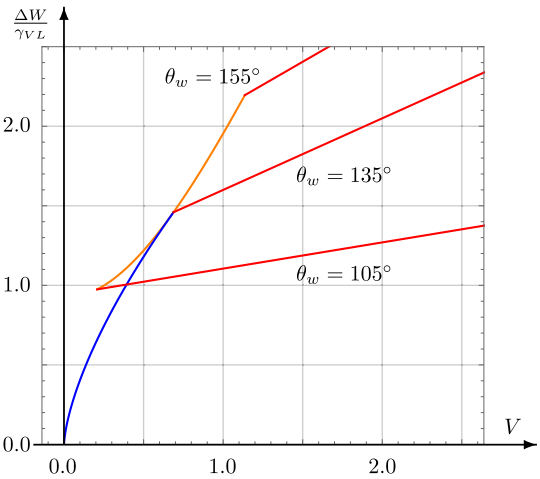

Figure 2. Illustration of the normalized surface energy for the CENTER (blue), INTERMEDIATE (orange), and COMPLETE (red) configurations for (θ_b, θ_w) = (45, 105°), (45, 135°), and (45, 155°) as a function of the droplet volume V. In the second case, because $\theta_m = \theta_M$, the INTERMEDIATE configuration does not exist. Results obtained for $R = h = 1$.

(normalized) surface energy of CENTER, INTERMEDIATE, and COMPLETE configurations as functions of the droplet volume for a cavity with $R = h = 1$ (aspect ratio 1) and three qualitatively different values for the pair (θ_b, θ_w), that is, (45, 105°), (45, 135°), and (45, 155°). In the first case, the upper limit value of the CENTER configuration is higher than the lower value of the COMPLETE configuration because we have $\theta_w - \pi/2 < \theta_b$. In the second case, the INTERMEDIATE configuration does not exist as we have exactly $\theta_w - \pi/2 = \theta_b$. In the third case, the INTERMEDIATE configuration connects the CENTER configuration to the COMPLETE configuration as $\theta_w - \pi/2 > \theta_b$. The case of a Ga droplet into a SiO_2/Si cylindrical cavity falls in the first class as $\theta_b = 50°$ and $\theta_w = 116°$.

For the EDGE and SIDE configurations, there are no explicit expressions for the areas that realize the minimum of the surface energy. Consequently, the corresponding surface energies were computed using the Surface Evolver software,[15,16] which minimize the total surface energy of a system subject to geometric and/or energetic constraints (see also ref 17).

3.1. Results for a Ga Droplet in a SiO_2/Si Cylindrical Cavity. Ga droplets wet Si(111) surfaces at wetting angles[a] $\theta_b = 50°$ and SiO_2 surfaces at $\theta_w = 116°$. Comparing the normalized surface energies, $E_{drop}/(A_{cav}\gamma_{LV})$ obtained for each configuration above allows one to determine as functions of the volume of the droplet and the cavity aspect ratio, the minimum surface energy, and thus the optimal morphology of the droplet. Figure 3 shows the normalized surface energies as a function of the (normalized) droplet volume in two generic situations: for $R/h = 1$ and for $R/h = 3.5$.

We notice that, independent on the aspect ratio, the EDGE configuration realizes the minimum surface energy at low volumes, while at large volumes the surface energy minimum is attained in the COMPLETE configuration. As shown in Figure 3, when the EDGE configuration exists it always has a lower surface energy than the CENTER configuration. Then, at a volume near the upper limit of existence (for instance, $V_{drop}/V_{cav} = 0.27$ for $R/h = 1$ and $V_{drop}/V_{cav} = 0.95$ for $R/h = 3.5$), the EDGE configuration surface energy becomes higher than that of the COMPLETE configuration, which increases slower than the others. We also notice in Figure 3 that the INTERMEDIATE configuration always has a higher energy than the CENTER, EDGE, and COMPLETE configurations. In all situations, we have studied that the surface energy of the SIDE configuration is extremely high so that for the sake of simplicity, we did not represent it in Figure 3b. This is a consequence of the important contact angle of the droplet with the wall $\theta_w = 116°$, so the SIDE configuration will not be considered any further.

Evolution of the EDGE configuration as a function of the droplet volume depends on the cavity aspect ratio. Figure 4 shows various droplet configurations for $R/h = 1$ (left sequence) and $R/h = 3.5$ (right sequence). Figure 3a shows that in the former case the maximum volume in the EDGE configuration is attained when $V = 0.29 \cdot V_{cav}$, while in the later for $V = 1.03 \cdot V_{cav}$, as shown in Figure 3b.

We conclude that, as a general rule, the volume of the Ga droplet should not be too low because the EDGE configuration is always the minimum surface energy configuration at low volumes. It is worth noticing that our results are significantly different from the results presented in ref 8 for the same contact angles and aspect ratio $R/h = 1$. More precisely, in ref 8 the authors concluded that at very low droplet volumes, the CENTER configuration has the lowest energy, then it is the EDGE configuration, and then the COMPLETE configuration. In contrast, we show here that the CENTER configuration never realizes the minimum energy morphology while the EDGE (at low droplet volumes) and the COMPLETE configurations (at large droplet volumes) are always preferred by the droplet. A careful analysis of the Supporting Information in ref 8 shows that this qualitative difference is related to the definition of the surface energy in ref 8 whose main drawback is that it does not tend to zero when the droplet volume tends to zero.

3.2. Dewetting Condition. In order to complete this study, various values of contact angles were also tested. An interesting result was obtained when the contact angles θ_w and θ_b satisfy the relation

$$\theta_w - \theta_b > \frac{\pi}{2} \tag{6}$$

In this case, initially placed in the EDGE configuration, the droplet leaves the sidewall of the cavity after a few iterations. This is the classical "dewetting" of the sidewall represented in Figure 5. The final minimum surface energy configuration is one when the droplet wets only the bottom of the cavity, which is a configuration similar to the CENTER one, except that, due to the initial condition in the minimization process, it is shifted toward the side of the cylinder base. The dewetting will be discussed further in Subsection 4.2. At first sight, this is a very interesting property for our applications as it should avoid initial tilted NW growth during the VLS process. Condition 6 is the same as the dewetting condition presented in ref 18 in the case of a droplet wetting two perpendicular planes.

4. DROPLET IN A CONICAL CAVITY

Although precise and complete, the previous results do not fit the experimental observations of the Ga droplets on patterned SiO_2/Si substrates. Indeed, for small volumes, the droplets are seen wetting only the bottom of the cavity but are not necessarily centered. This seems contradictory with the results previously

https://doi.org/10.1021/acs.cgd.2c00685
Cryst. Growth Des. XXXX, XXX, XXX−XXX

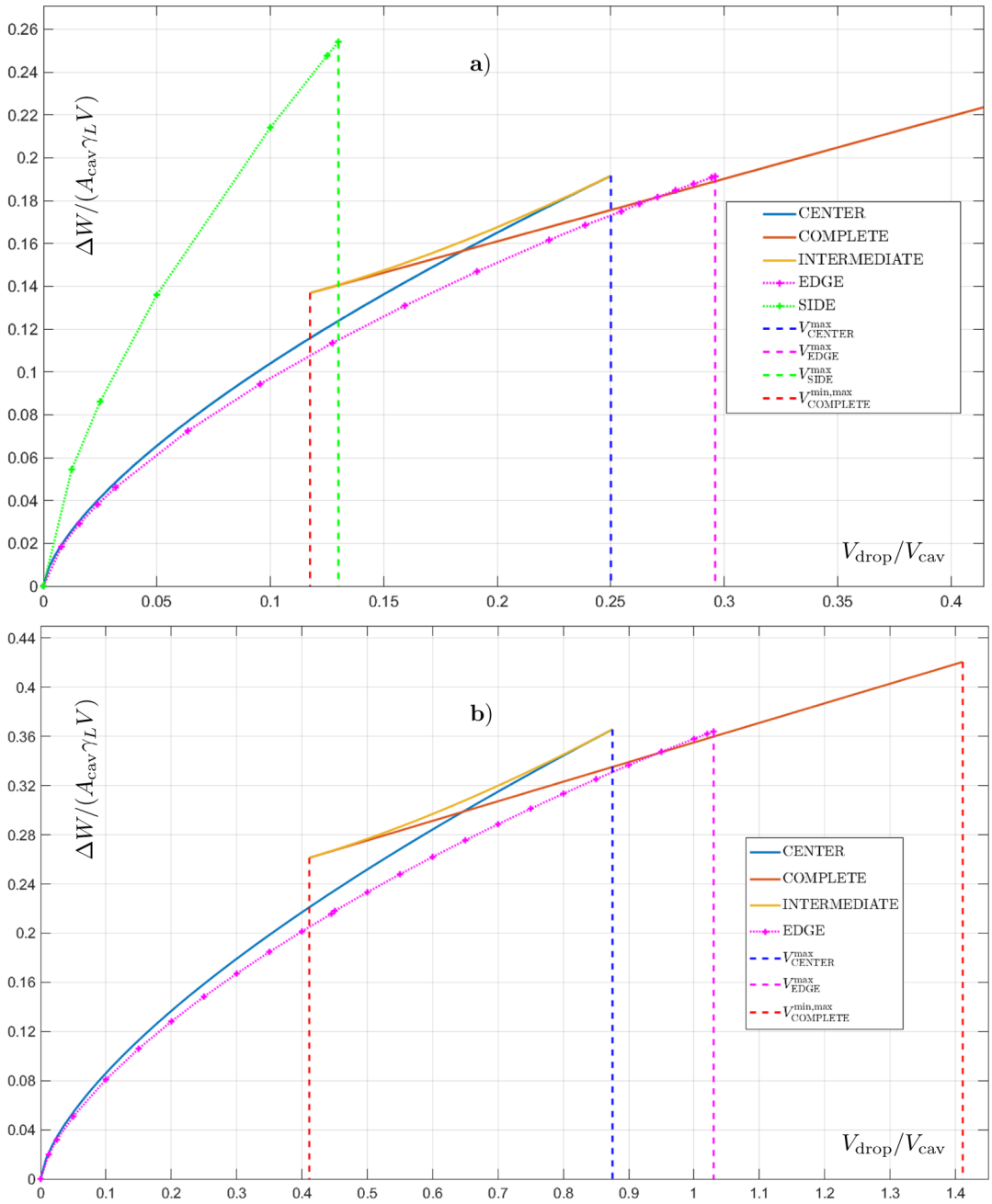

Figure 3. (a) Energies of the different configurations for an aspect ratio $R/h = 1$ as a function of the normalized droplet volume. In full lines: the energies were calculated analytically. In dashed lines: the energies for the SIDE and EDGE configurations computed using Surface Evolver. (b) Same as (a) but for $R/h = 3.5$. The SIDE configuration energy is not represented here due to its higher energy.

presented as the droplet is expected to wet on the edge of the cavity, that is, a part of the bottom and a part of the side. However, it is also known that the cavities in the SiO_2/Si substrate are not exactly cylindrical (see ref 12). The process of creation of the cavities involves a treatment of the surface with fluorhydric acid to remove the remaining SiO_2 at the bottom of the cavities. Altogether, the resulting cavities have the shape of a truncated cone with an opening angle $\alpha \simeq 28°$, as shown in Figure 6. Thus, in addition to the aspect ratio R/h, the truncated cone cavities have an additional geometric parameter: the opening angle α.

In this part, all the configurations are defined in the same way as for the cylindrical cavity. The main modification is that the sidewall of the cavity is not a cylinder but a truncated cone. The CENTER configuration is not modified as it is independent from the wall of the cavity. New formulas are needed for the COMPLETE configuration and the EDGE and SIDE configurations, which were studied numerically. For the INTERMEDIATE configuration, the formulas are still the same but the limit angles of existence θ_1 and θ_2 are modified. The tilt of the sidewall introduces a new angle, further denoted as θ_{cw} (for *conical wall*), and defined as

$$\theta_{cw} = \theta_w + \alpha - \frac{\pi}{2} \tag{7}$$

Thus, the new limit angles are now $\theta_1 = \min(\theta_b, \theta_{cw})$ and $\theta_2 = \max(\theta_b, \theta_{cw})$. With our values, that is, $\theta_b = 50°$, $\theta_w = 116°$, $\alpha = 28°$ (from ref 12), we obtain $\theta_{cw} = 54°$ and thus $\theta_1 = \theta_b$ and $\theta_2 =$

https://doi.org/10.1021/acs.cgd.2c00685
Cryst. Growth Des. XXXX, XXX, XXX−XXX

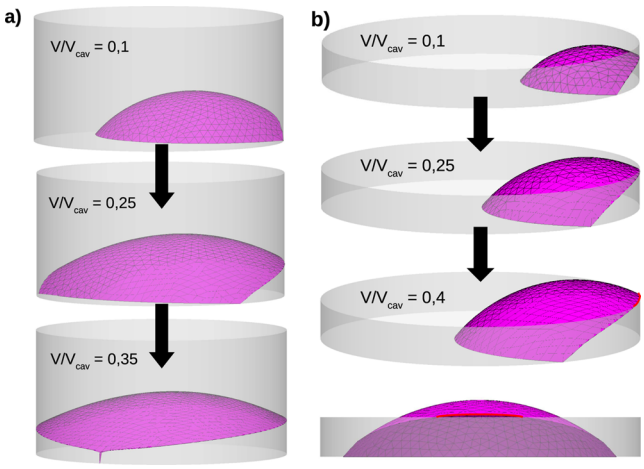

Figure 4. Evolution of the EDGE configuration as a function of V/V_{cav}: (a) for $R/h = 1$ the droplet progressively wets along the sidewall, until all the bottom of the cavity is covered. The corresponding volume is referred to as V^{max}_{EDGE} in Figure 3a. For $R/h = 1$, $V^{max}_{EDGE} = 0.29$. (b) For a high aspect ratio (here $R/h = 3$), when the highest point of the droplet reaches the top of the cavity at $V/V_{cav} = 0.35$, the droplet will share a common boundary with the upper surface of the cavity and spread along the upper edge of the cavity until a maximum volume value (i.e., 1.03 in Figure 3b that depends on both wetting angles θ_b and θ_w).

θ_{cw}. This is different from the cylindrical cavity, where θ_b was the maximal value of θ_i. Now, it is the minimum value, so that we notice that in this case, the opening of the truncated cone induces an inversion of the θ_i bounds.

4.1. Results for a Ga Droplet in a Conical Cavity with an Angle α = 28°. The main result concerns the evolution of a droplet initially placed in the EDGE configuration. Contrary to the results obtained for the cylindrical cavity, the contact angles of a Ga droplet wetting Si on the bottom of the cavity and SiO_2 on the sidewall, with $\alpha = 28°$, lead to a systematic dewetting from the sidewall of the cavity. As long as the volume of the droplet is small enough not to wet all the bottom of the cavity, the droplet in the EDGE configuration always leaves the sidewall to wet only the bottom, thus being in a configuration similar to the CENTER one but not centered inside the cavity, as shown Figure 7a,b. The energies of the different configurations are shown in Figure 7c (except as previously for the SIDE configuration, due to its much higher energy).

At low volumes, the energy of the EDGE configuration is equal to the one of the CENTER configuration. This is indeed coherent with the dewetting observed: the droplet only wets the bottom of the cavity with the angle θ_b, being in the CENTER configuration but shifted toward the corner due to its initial position. Once V^{max}_{CENTER} is passed, the droplet adopts the INTERMEDIATE configuration. It wets the whole bottom of the cavity and the contact angle varies from $\theta_b = 50°$ to (see Figure 7) $\theta_{cw} = 54°$. Like smaller droplets, the EDGE droplet in

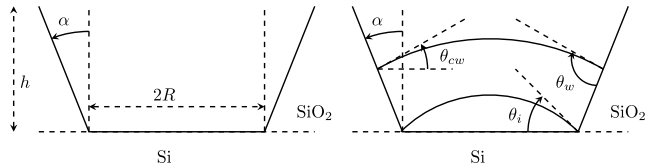

Figure 6. Left: geometric parameters in the vertical section of the truncated cone: angle α, basis radius R, and a height h. Right: illustration of the droplet with the angle $\theta_{cw} = \theta_w + \alpha - \pi/2$.

this interval of volume totally dewets the sidewall of the cavity, now wetting the whole bottom as in the INTERMEDIATE configuration; hence, the equality of the energies noted in Figure 7. Beyond $V^{max}_{INTER} = V^{min}_{COMPLETE}$, the EDGE configuration does not exist anymore. The volume is such that the droplet is forced to wet the sidewall because all the bottom is wet with the maximum possible contact angle.

Consequently, for a realistic conical cavity, our conclusions for the Ga droplet is that at low volumes, it wets the bottom of the cavity only, until the maximal volume which can be put in the bottom is reached. Then, the droplet adopts the only configuration possible, that is, the COMPLETE one, wetting the whole bottom and also a part of the sidewall, symmetrically. Other similar calculations and measurements with the same angles but with different aspect ratios (not shown here) confirm this dewetting of this sidewall dewetting phenomenon, when the volume is low enough. It should be noted that this result is actually independent of the aspect ratio of the cavity.

4.2. Generalized Dewetting Condition. In this subsection, we generalize the dewetting conditions obtained in Subsection 3.2 in a particular case. Taking into account the new geometric parameter of the conical cavity, that is, the angle α, we conclude that the dewetting from the sidewall occurs when the opening of the truncated cone, that is, α is large enough. This condition reads

$$(\theta_w + \alpha) - \theta_b > \frac{\pi}{2} \tag{8}$$

With the numerical values for a Ga droplet in a SiO_2/Si cavity, with $\theta_b = 50°$ and $\theta_w = 116°$, relation 8 is equivalent to

$$\alpha > \frac{\pi}{2} + \theta_b - \theta_w = 24° \tag{9}$$

Thus, for conical cavities on SiO_2/Si with an angle greater than 24°, we should observe a dewetting similar to the one described in Subsection 4.1. For the later, the dewetting condition was indeed full-filled for $\alpha = 28° > 24°$. Other tests were conducted with the same contact angles but with a greater α, for instance $\alpha = 40°$. Accordingly to our condition, we observed systematic dewetting too, independently from the aspect ratio.

Values of α below 24° were also tested: numerical results for $\alpha = 20°$ are shown in Figure 8 where the considered values of θ_b

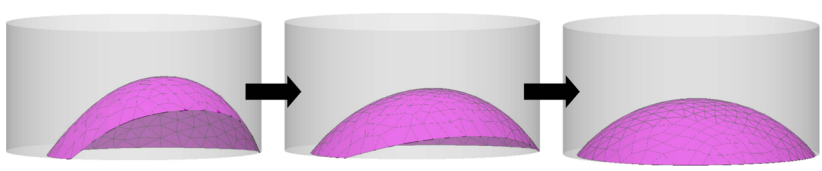

Figure 5. Configurations corresponding to different iterations with Surface Evolver showing progressive dewetting of the drop for $V/V_{cav} = 0.2$ and an aspect ratio of 2. Here, $\theta_b = 50°$, $\theta_w = 150°$ so 6 is fulfilled.

https://doi.org/10.1021/acs.cgd.2c00685
Cryst. Growth Des. XXXX, XXX, XXX−XXX

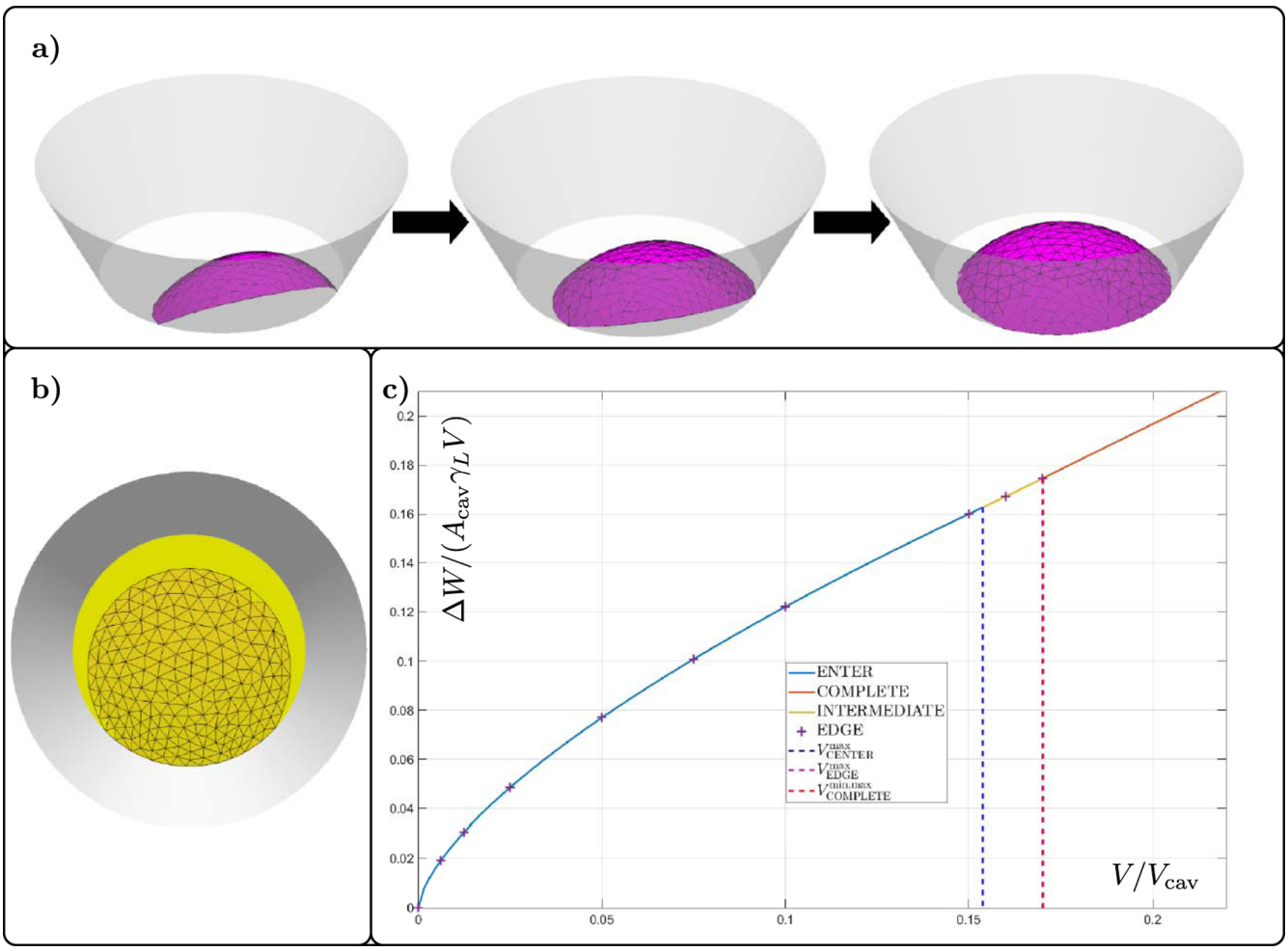

Figure 7. (a) Ga droplet dewetting the sidewall, for $R/h = 1$ and $V/V_{cav} = 0.1$. (b) Top view of the droplet once it has totally dewet the sidewall (here the droplet is transparent and in yellow, we represent the bottom of the cavity; the sidewall are represented in gray). (c) Energies of the different configurations, for aspect ratio $R/h = 1$.

and θ_w were the same as previously reported. In Figure 8a,b, the droplet in the EDGE configuration still wets a small part of the sidewall after the iterations: there is no total dewetting, as expected from relation 9. The energy landscape shown in Figure 8c shows that the energy of the EDGE configuration is very close to those of the other configurations (because the droplet has almost left the sidewall), but still it is always slightly lower. The behavior of the droplet is then hard to predict due to the tiny difference in surface energies, but the minimum energy configuration is, as in the cylindrical case, the EDGE configuration at low volume and then at larger volumes, the COMPLETE one.

The experimental angle $\alpha = 28°$ should lead to systematic dewetting from the sidewall and thus to a vertical growth, at least as long as the volume of liquid Ga is not too high. However, this angle is very close to the limit angle 24° so that small variations around this angle (due, for instance, to uncertainties on the contact angles of the droplet on the bottom and on the sidewall or due to cavity defects) could explain the low proportion of tilted NWs we still observe.

The modeled dewetting actually corresponds quite well to what we have observed and reported in ref 12. In those experiments, GaAs NWs were grown by molecular beam epitaxy (MBE) on SiO_2/Si(111) patterned substrates with conical cavities in the SiO_2 layer (typically 20 nm thick) fabricated by electron-beam lithography and etching (more details on the growth conditions can be found in ref 12). Then, transmission electron microscopy images were performed on different epitaxial NWs (see Figure 9). Interestingly, while most of NWs grew vertically (as the one visible in Figure 9a), some of them exhibit an inclined growth direction (Figure 9b). The angle α formed by the facets of the GaAs NW and the normal to the Si surface is in the range (26, 30°) (near the bottom of the cavity) in Figure 9a and in the range (22, 23°) (near the bottom of the cavity) in Figure 9b, respectively, in good agreement with our numerical estimates.

It is also interesting to notice that experimental observations indicate that accidentally, the orientation of the lateral surface of cavities in SiO_2 is not constant, which is a situation not covered by our results. Nevertheless, the above results allow one to speculate that in conical cavities with non-constant sidewall inclination the Ga droplets will wet the sidewall of the cavity at different heights, so that in that case the triple line is not planar. As a consequence, a part of the triple line will attain the border of the cavity although the remaining part still wets the sidewall of the cavity leading to inclined NW growth. This scenario and our previous results point out the importance of the geometry of the cavity as well as its homogeneity in order to improve verticality.

https://doi.org/10.1021/acs.cgd.2c00685
Cryst. Growth Des. XXXX, XXX, XXX−XXX

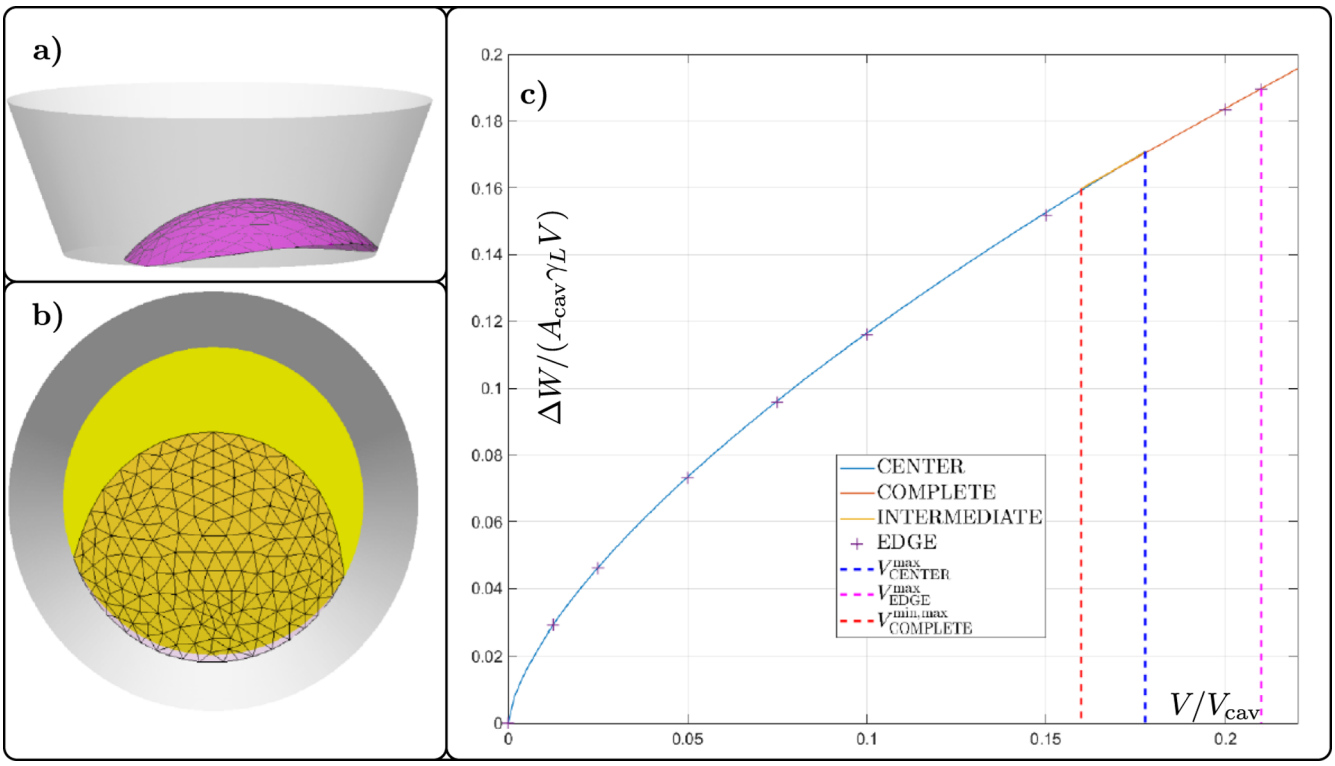

Figure 8. (a) With $\alpha = 20°$, the Ga droplet in the EDGE configuration still wets a part of the sidewall, for $R/h = 1$ and $V/V_{cav} = 0.1$. (b) Top view of the same droplet (the droplet is transparent. In yellow: the bottom of the cavity; in grey: the sidewall). (c) Energies of the different configurations, for $R/h = 1$. The tiny difference between the EDGE energy and the CENTER and COMPLETE ones can be noticed in the figure (red crosses are always lower that the blue and orange curves).

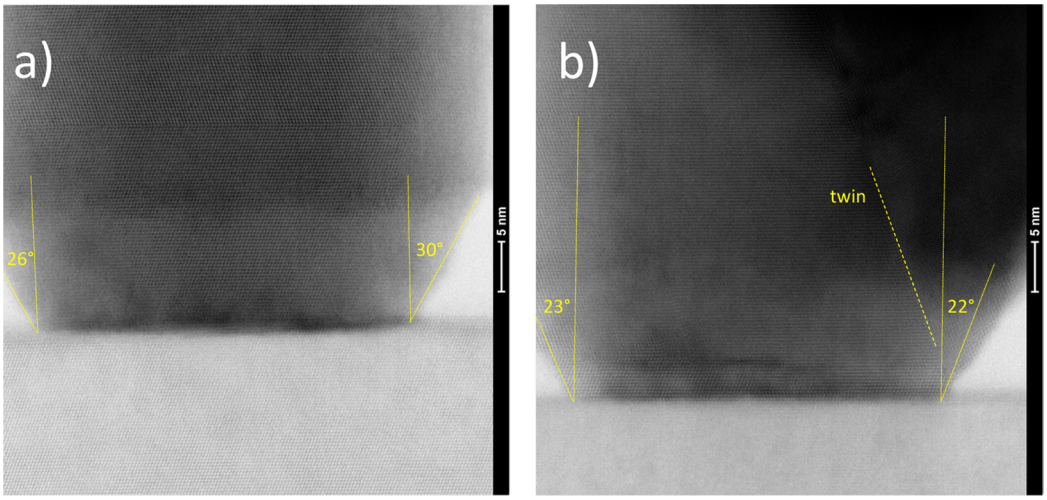

Figure 9. (a) Transmission electron microscopy images (with $[1\bar{1}0]$ zone axis) of GaAs NWs grown by MBE on conical cavities. In (a), the NW grew vertically due to a high value of the α angle [in the range (26, 30°)] while in (b), the GaAs NW did not grow vertically due to the low value of the α angle here 22−23° near the bottom of the cavity and non-constant sidewall inclination (non-uniformity). Notice that: in (a) the normal direction to the substrate is slightly inclined (to the left) in the TEM image and in (b) the indicated twins seem to be corelated to the change in the sidewall inclination.

5. CONCLUSIONS

As the initial step of the NW growth process involves droplets in various cavities, the analysis of the minimal surface energy configurations of a droplet in a cavity becomes an important factor to control the NW verticality.

We compute and compare the surface energy of morphologically different configurations for droplets wetting a cylindrical cavity in situations, in which the wetting angle on the bottom of the cavity and the wetting along the sidewall are different. Depending on the aspect ratio of the cylindrical cavity, defined here as radius/height, some of these configurations can exist only in some specific droplet volume intervals. We find that as a general rule, the EDGE configuration realizes the minimum surface energy for small droplet volumes, while the COMPLETE configuration is the minimum surface energy for large droplet volumes. An important feature of the EDGE configuration is that the triple line (contact between the droplet and the sidewall and/or bottom of the cavity) is not planar, as it

https://doi.org/10.1021/acs.cgd.2c00685
Cryst. Growth Des. XXXX, XXX, XXX−XXX

seems to be also the case when the inclination of the lateral walls is not constant. In these configurations, evolution of the NW is such that the higher part of the triple line reaches the top of the cavity while the remaining part still wets the sidewall leading to an inclined NW growth. For simplicity and in order to compare our results to those obtained using a similar procedure in ref 8, we used all along this study for the wetting angles θ_b (between the Ga droplet and the Si substrate) and θ_w (the angle between the droplet and the side-walls) the same numerical values as in ref 1. However, it is known that the characterization of the surface energy using the wetting angles is a practical simplification of a more complex physical context that may involve other significant material parameters. As a consequence, a natural question concerns the stability of our results with respect to variations of the wetting angles. Toward an answer to this, we can only argue that the minimization procedure provides a generic situation which remains stable with respect to (small) variations of the wetting angles around the values considered in this study. A larger scale study of the qualitative aspects related to this issue will be the subject of a future work.

From a more general perspective, depending on the values of the wetting angles on the bottom of the cavity and on the sidewall, we notice that dewetting on the sidewall of a cylindrical cavity takes place when the condition $\theta_w - \theta_b > \pi/2$ is full-filled. Control of the dewetting of the sidewall of the cavity is very important for the NW growth and in particular to improve the verticality. Taking the above inequality as a starting point, we extend our result to cover also the wetting of a conical cavity, in which case the geometry of the cavity has an additional geometric parameter, the opening angle α. We show that dewetting on the sidewall for a conical cavity occurs when $\theta_w + \alpha - \theta_b > \pi/2$ an inequality that generalizes that obtained for cylindrical cavities.

An interesting perspective of this study that we will address in a future work is the wetting in conical cavities with orientation-dependent inclination. The main difficulty in this case is the choice among all possible configurations of those pertinent to NW growth applications.

AUTHOR INFORMATION

Corresponding Author

Alexandre Danescu − *University of Lyon, Institute of Nanotechnologies de Lyon—INL, UMR CNRS 5270, Ecole Centrale de Lyon, 69130 Ecully, France*; Email: alexandre.danescu@ec-lyon.fr

Authors

Louis Bailly-Salins − *University of Lyon, Institute of Nanotechnologies de Lyon—INL, UMR CNRS 5270, Ecole Centrale de Lyon, 69130 Ecully, France;* Present Address: Laboratoire de Physique Corpusculaire, ISMRA, IN2P3-CNRS et Université de Caen, 14050 Caen Cédex, France

Marco Vettori − *University of Lyon, Institute of Nanotechnologies de Lyon—INL, UMR CNRS 5270, Ecole Centrale de Lyon, 69130 Ecully, France;* Present Address: Department of Applied Physics, Eindhoven University of Technology, Groene Loper 19, 5612AP Eindhoven, The Netherlands.

Thomas Dursap − *University of Lyon, Institute of Nanotechnologies de Lyon—INL, UMR CNRS 5270, Ecole Centrale de Lyon, 69130 Ecully, France*

Philippe Regreny − *University of Lyon, Institute of Nanotechnologies de Lyon—INL, UMR CNRS 5270, Ecole Centrale de Lyon, 69130 Ecully, France*

Gilles Patriarche − *Centre de Nanosciences et de Nanotechnologies—C2N, CNRS, Université Paris-Sud, Université Paris-Saclay, 91120 Palaiseau, France;* orcid.org/0000-0002-3917-2470

Michel Gendry − *University of Lyon, Institute of Nanotechnologies de Lyon—INL, UMR CNRS 5270, Ecole Centrale de Lyon, 69130 Ecully, France*

José Penuelas − *University of Lyon, Institute of Nanotechnologies de Lyon—INL, UMR CNRS 5270, Ecole Centrale de Lyon, 69130 Ecully, France;* orcid.org/0000-0002-5635-7346

Complete contact information is available at: https://pubs.acs.org/10.1021/acs.cgd.2c00685

Notes

The authors declare no competing financial interest.

ACKNOWLEDGMENTS

We acknowledge funding from the projet ANR-15-CE05-0009 HETONAN. We also acknowledge Prof K. Brakke for his prompt answering and precious insights regarding the implementation of constraints in Surface Evolver (ref 15).

ADDITIONAL NOTE

[a]Obviously, these numerical values should be carefully considered since their precise measurement is difficult. Hereafter, for practical purposes in our numerical investigation, we used these values but, obviously, all our results can be adapted to different numerical data.

REFERENCES

(1) McIntyre, P. C.; Fontcuberta i Morral, A. Semiconductor nanowires: to grow or not to grow? *Mater. Today Nano* **2020**, *9*, 100058.

(2) Wagner, R. S.; Ellis, W. C. Vapor-Liquid-Solid Mechanism of Single Crystal Growth. *Appl. Phys. Lett.* **1964**, *4*, 89.

(3) Fouquat, L.; Vettori, M.; Botella, C.; Benamrouche, A.; Penuelas, J.; Grenet, G. X-ray photoelectron spectroscopy study of Ga nanodroplet on silica terminated silicon surface for nanowire growth. *J. Cryst. Growth* **2019**, *514*, 83−88.

(4) Ra, Y.-H.; Rashid, R. T.; Liu, X.; Lee, J.; Mi, Z. Scalable Nanowire Photonic Crystals: Molding the Light Emission of InGaN. *Adv. Funct. Mater.* **2017**, *27*, 1702364.

(5) Vukajlovic-Plestina, J.; Kim, W.; Dubrovski, V. G.; Tütüncüoğlu, G.; Lagier, M.; Potts, H.; Friedl, M.; Fontcuberta i Morral, A. Engineering the Size Distributions of Ordered GaAs Nanowires on Silicon. *Nano Lett.* **2017**, *17*, 4101.

(6) Kinge, S.; Crego-Calama, M.; Reinhoudt, D. N. Self-Assembling Nanoparticles at Surfaces and Interfaces. *ChemPhysChem* **2008**, *9*, 20.

(7) Demontis, V.; Zannier, V.; Sorba, L.; RossellaSorba, F. Surface Nano-Patterning for the Bottom-Up Growth of III-V Semiconductor Nanowire Ordered Arrays. *Nanomaterials* **2021**, *11*, 2079.

(8) Vukajlovic-Plestina, J.; Kim, W.; Ghisalberti, L.; Varnavides, G.; Tütüncuoglu, G.; Potts, H.; Friedl, M.; Güniat, L.; Carter, W. C.; Dubrovskii, V. G.; Fontcuberta i Morral, A. Fundamental aspects to localize self-catalyzed III-V nanowires on silicon. *Nat. Commun.* **2019**, *10*, 869.

(9) Yuan, X.; et al. Role of surface energy in nanowire growth. *J. Phys. D: Appl. Phys.* **2018**, *51*, 283002.

(10) Harmand, J.-C.; et al. Atomic Step Flow on a Nanofacet. *Phys. Rev. Lett.* **2018**, *121*, 166101.

(11) Maliakkal, C. B.; Tornberg, M.; Jacobsson, D.; Lehmann, S.; Dick, K. A. Vapor−solid−solid growth dynamics in GaAs nanowires. *Nanoscale Adv.* **2021**, *3*, 5928.
(12) Vettori, M.; Piazza, V.; Cattoni, A.; Scaccabarozzi, A.; Patriarche, G.; Regreny, P.; Chauvin, N.; Botella, C.; Grenet, G.; Penuelas, J.; Fave, A.; Tchernycheva, M.; Gendry, M. Growth optimization and characterization of regular arrays of GaAs/AlGaAs core/shell nanowires for tandem solar cells on silicon. *Nanotechnology* **2019**, *30*, 084005.
(13) Matteini, F.; et al. Impact of the Ga Droplet Wetting, Morphology, and Pinholes on the Orientation of GaAs Nanowires. *Cryst. Growth Des.* **2016**, *16*, 5781.
(14) Gibbs, J. W. *The Scientific Papers of J. Willard Gibbs: In Two Volumes*; Ox Bow Press: Woodbridge, CT, 1993; Vol. *1*.
(15) Brakke, K. A. The Surface Evolver. http://facstaff.susqu.edu/brakke/evolver/evolver.html, accessed 28/4/2022.
(16) Brakke, K. A. The Surface Evolver. *Exp. Math.* **1992**, *1*, 141.
(17) Brakke, K. A. *Surface Evolver Manual*; Susquehanna University, 2013.
(18) Berthier, J.; Brakke, K. A. *The Physics of Microdroplets*; John Wiley & Sons; Scrivener Publishing LLC: Hoboken, NJ; Salem, MA, 2012; p 556.

https://doi.org/10.1021/acs.cgd.2c00685
Cryst. Growth Des. XXXX, XXX, XXX−XXX